CONCEPTUAL DESIGN AND PERFORMANCE ANALYSIS SOFTWARE TOOL FOR ROTORCRAFT SYSTEMS

Tomás Figueiredo Ventura Pimentel Fontes, tomas.fontes@tecnico.ulisboa.pt, Instituto Superior Técnico, Universidade de Lisboa (Lisboa, Portugal)

Filipe Szolnoky Ramos Pinto Cunha, filipescunha @tecnico.ulisboa.pt, IDMEC, Instituto Superior Técnico, Universidade de Lisboa (Lisboa, Portugal)

Abstract

The availability of a free open source tool for the design and performance evaluation of rotary wing aircrafts is scarce, this work intends to provide a solution for engineering students, aircraft engineers or anyone interested in aircraft design with such a tool. The tool applies the Momentum theory and the Blade Element theory to execute the analysis of the rotor performance and presents the results in a clear and simple way (power against airspeed plots, rotor disk distribution plots of the calculated variables, as well as numerical results explicitly identified). A small data base with airfoils (and their aerodynamic performances) is included in the tool. The tool's results validation is done and presented to assure the user of the reliability of the analyses done.

1. INTRODUCTION

1.1. Motivation

A helicopter is an aircraft that uses rotary wing systems (rotors) to produce lift, thrust and control forces. This generation of force does not require forward velocity, so the aircraft can lift vertically and hover. Motion can be induced by tilting the rotor, depending on the direction of this action the helicopter can move forwards or backwards, left or right. The wide range of flight movements even at low speeds give the helicopter characteristics like no other aircraft making it suitable for all kinds of operation.

Versatility doesn't come without a cost, for this kind of aircraft can operate under very different flight conditions, each having specific requirements, making it delicate (or near impossible) to have an optimal performance for all the different design points (hovering, cruise flight, maximum speed flight, climb). Rotorcraft design is a multidisciplinary problem that includes fields as aerodynamics, aeroelasticity, thermodynamics, structures and materials, flight dynamics and controls.

Many software tools for conceptual and preliminary rotorcraft design have been developed throughout the last 40 to 50 years, but a free and open source tool is still not easy to come across. The work developed here aims to provide such a tool for anyone interested in rotary wing aircrafts' design.

The simple and direct nature of the MatLab tool will allow the user to easily make design modifications and calculate their impact on the aircraft performance as to verify theoretical concepts, empirical models or any other performance related aspect of the rotorcraft.

1.2. Previous projects

A lot of rotorcraft design tools have been developed throughout the years to evaluate flight performance (considering rotor and fuselage aerodynamics, structural and weight analysis, and control and stability), environmental impact (fuel consumption, noise, and exhaust gas emissions) and aircraft manufacturing, maintenance and operational costs.

Previous to this work several tools were already developed in Instituto Superior Técnico. Roman Vasyliovych Rutsky [1], developed a tool for the preliminary design of a conventional helicopter, Anatol Conjocari [2], expanded the tool to other helicopters configurations (co-axial and tandem), and Miguel Ponte [3], further developed the complexity of the tool introducing the possibility of a more detailed rotor blade design (airfoil change along the blade, as well as chord and twist distributions).

Amongst the available commercial tools, for example, the work developed by the Israel Institute of Technology RAPID/RaTE can be mentioned, wihch is a software package for rotorcraft preliminary design analysis, it models general

Presented at 46th European Rotorcraft Forum, Moscow, Russia, 8-11 September, 2020

configurations (conventional helicopters and tilt-rotors) based on existing aircrafts by extracting common features, or "design trends", which are then used in the first sizing stage of the helicopter design, later it performs trim response, mission, vibration, and stability analysis as well as flight mechanics and aeroelastic simulations, see [4].

2. THEORETICAL BACKGROUND

Two main theories are available to evaluate the helicopter rotor's performance, the Momentum Theory (MT), and the Blade Element Theory (BET). Each of these theories will be described in this section following the content presented in [5].

2.1. Momentum Theory

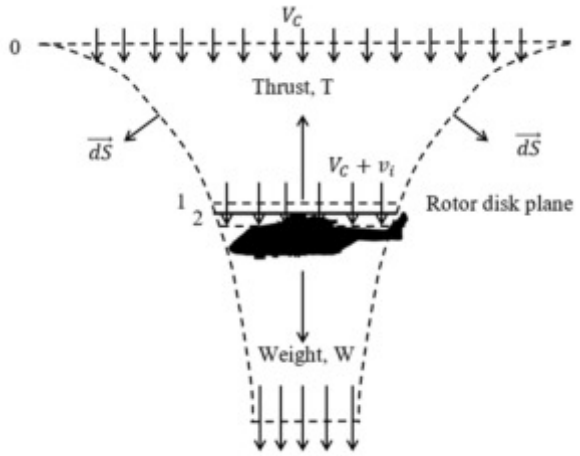

Figure 1: Flow model for momentum theory in hovering flight

The generic approach of this problem assumes that the flow is one-dimensional, quasi-steady, incompressible and inviscid, and although it does not take into account the complex vortical wake structure associated with the rotor aerodynamics or the actual details of the flow environment (local flow around the rotor blade), it allows for a first-order prediction of the thrust generated and power required for a given flight condition.

Applying basic conservation laws of fluid mechanics to the control volume of Figure 1 (such as conservation of mass, equation 1, momentum, equation 2 and energy, equation 3) to the rotor flow, as a whole, estimations of the performance can be made, this simple approach became known as the Rankine-Froude momentum theory.

(1) $\int\int_S \rho\,\vec{V}.\overrightarrow{dS} = 0$

where ρ is the specific mass, $\vec{V}$ the flow velocity, and $\overrightarrow{dS}$ the unit vector normal to the control volume surface S.

(2) $\int\int_S p\overrightarrow{dS} + \int\int_S (\rho\vec{V}.\overrightarrow{dS})\vec{V} = \vec{F}$

where p is the pressure and $\vec{F}$ the resultant force.

(3) $\int\int_S \frac{1}{2}(p\,\vec{V}.\overrightarrow{dS})\left|\vec{V}\right|^2 = E$

where E is the work done on the fluid by the rotor.

Applying these three equations for the different flight conditions stages (typically hover, axial climb and level flight) a series of relations can be derived for the analysis and comprehension of the helicopter characteristics.

2.2. Blade Element Theory

Rotor aerodynamics analysis has its foundation on Blade Element Theory as is allows to calculate radial and azimuthal distributions of the aerodynamic loads over the rotor disk. The base assumption of this theory is that each blade section acts as a 2D airfoil to produce forces. The rotor performance is calculated integrating the airloads of each section along the blade and averaging the results over a complete revolution. This theory, unlike the momentum theory, can be used as a basis to design the rotor blade in terms of twist and chord distribution, as well as in terms of the airfoil, or airfoils, to be used.

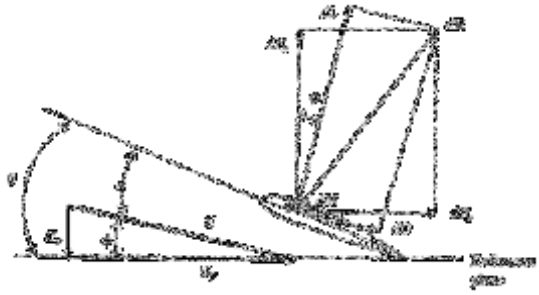

Figure 2: Blade element - Force diagram

In Figure 2 α is the angle of attack, ϕ the inflow angle, and θ the blade section pitch angle.

The force analysis gives us:

(4) $dL = \frac{1}{2}\rho U^2 c C_l dy$, and $dD = \frac{1}{2}\rho U^2 c C_d dy$

where L is the aerodynamic lift, U the inflow velocity, c the blade chord, C_l the airfoil lift coefficient, D the aerodynamic drag and C_d the airfoil drag coefficient.

The forces aligned with the perpendicular (z) and parallel (x) directions (in relation with the rotor plane) can be expressed:

(5) $dF_z = dL\cos\phi - dD\sin\phi$, and $dF_x = dL\sin\phi + dD\cos\phi$

And consequently the thrust, T, torque, Q, and

Presented at 46th European Rotorcraft Forum, Moscow, Russia, 8-11 September, 2020

power, P, contributions are:

(6) $dT = N_b dF_z$, $dQ = N_b dF_x y$, and $dP = N_b dF_x \Omega y$

with N_b being the rotor number of blades.

2.3. Linear inflow models

When considering a forward flight condition, the assumption of axisymmetric flow is not valid, nonetheless simple models can be used to estimate the basic effects of the inflow. The simplicity of these models has made them widely used in helicopter rotor aerodynamics problems.

The general form of these models is:

(7) $\lambda_i = \lambda_0 \, (1 + k_x r cos\Psi + k_y r sin\Psi)$

with λ_i being the inflow ratio at a given position, k_x and k_y are, respectively, the longitudinal and lateral inflow slopes, r is the nondimensional radial position and Ψ is the azimuthal coordinate. λ_0 is the inflow ratio at the center of the rotor.

The different models considered in this work are as follows:

- Coleman et al. (1945), [6]

(8) $k_x = \tan(\chi/2)$, and $k_y = 0$

- Drees (1949), [7]

(9) $k_x = (4/3)\,(1 - cos\chi - 1.8\mu^2)/sin\chi$

(10) $k_y = -2\mu$

- Payne (1959), [8]

(11) $k_x = (4/3)[\mu/\lambda(1.2 + \mu/\lambda)]$, and $k_y = 0$

- White & Blake (1979), [9]

(12) $k_x = \sqrt{2} sin\chi$, and $k_y = 0$

- Pitt & Peters (1981), [10]

(13) $k_x = (15\pi/23)(tan\chi/2)$, and $k_y = 0$

- Howlett (1981), [11]

(14) $k_x = \sin^2 \chi$, and $k_y = 0$

where χ is the wake skew angle and μ is the advance ratio.

2.4. Flapping blade

The motion resulting from the coupling of aerodynamic forces acting on the rotor is paramount to the understanding of the blade motion as to allow for the pilot to successfully control the helicopter. Rotors commonly have articulations near the blade root in the form of flapping and lead-lag hinges.

The equilibrium position of a flapping blade will depend on the relation between aerodynamic and centrifugal forces.

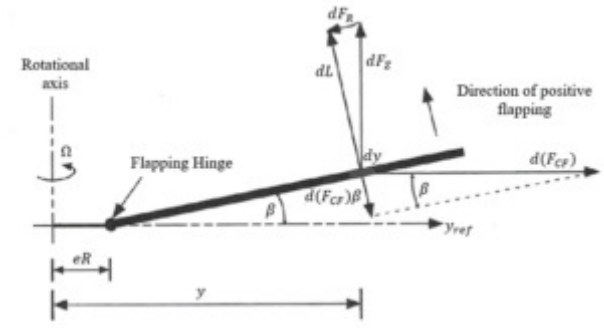

Figure 3: Blade forces equilibrium about the flapping hinge, small angle approximation

The equation of motion for a flapping blade results in:

(15) $\ddot{\beta} + \nu_\beta^2 \beta = \frac{1}{I_b \Omega^2} M_\beta$

with β being the flapping angle, $\ddot{\beta}$ its second derivative in respect to the azimuth angle, ν_β the nondimensional flapping frequency, I_b the mass moment of inertia, Ω the blade rotational velocity and M_β the aerodynamic moment.

The flapping motion is directly linked with the pilot's controls, if the pitch control is assumed to have a cyclic behaviour is relation to the azimuthal position then the flapping angle will have an analogous form. When both are approximated by their first terms of their harmonic series they can be represented as follows:

(16) $\theta(r, \Psi) = \theta_{tw}(r) + \theta_0 + \theta_c \, cos\Psi + \theta_s \, sin\Psi$

And:

(17) $\beta(\Psi) = \beta_0 + \beta_{1c} \, cos\Psi + \beta_{1s} \, sin\Psi$

where θ is the blade pitch, θ_{tw} is the blade twist, θ_c the longitudinal cyclic pitch and θ_s the lateral cyclic pitch. β_0, β_{1c} and β_{1s} are the components of the resulting expression for the flapping angle.

2.5. Prandtl's tip-loss function

Prandtl formalized a solution for the induced effects associated with a finite number of blades and with the effect of the blade tip (and to the same degree with the effect of the blade root), where the

Presented at 46th European Rotorcraft Forum, Moscow, Russia, 8-11 September, 2020

lift tends to zero. This solution takes into account the number of blades, the radial position of the element to be considered and the local inflow angle, see [5].

The correction factor, F, is expressed as:

(18) $F = \left(\frac{2}{\pi}\right)\cos^{-1} e^{f}$

where $f = f_{root}f_{tip}$ is dependent on the number of blades and radial position:

(19) $f_{tip} = \frac{N_b}{2}\left(\frac{1-r}{r\phi}\right)$, and $f_{root} = \frac{N_b}{2}\left(\frac{r}{(1-r)\phi}\right)$

where $r = y/R$ is the adimensional radial position, and ϕ is in radians.

2.6. Compressibility corrections to rotor performance

Over the rotor disk, depending on the flight conditions, higher Mach numbers may be reached, this will have a considerable impact on the produced aerodynamic forces so it becomes capital to take into account compressibility corrections. Glauert's rule, see [5], states that:

(20) $C_{l_\alpha} = \frac{C_{l_\alpha}|_{M=0.1}}{\sqrt{1-M^2}}$

where $C_{l_\alpha}|_{M=0.1}$ is the 2D lift-curve-slope at $M = 0.1$ and M is the local Mach number.

3. SOFTWARE IMPLEMENTATION

The computational tool is intended to allow the user to make the conceptual and preliminary design of a rotary wing aircraft (conventional, co-axial or tandem helicopters) at two different levels of complexity, these will be henceforth called the *basic design* and the *detailed design.* Additionally another tool was developed to the design of small dimensions unmanned rotorcrafts, *drone tool*. One peripheral tool was programmed so that the user could compare airfoil performances when designing the rotor blades *airfoil comparison tool*.

The main idea that dictates the behaviour of the tools is that the user defines the flight conditions (and top level aircraft requirements, in the *detailed tool*) in which the aircraft is to operate and calculations are made in order to assess the feasibility of the design. The user will have the freedom to conduct alterations (namely to the rotor geometry) and compare the performances of the different designs.

3.1. Basic tool

The information flow and user experience will be described in this chapter. First the user will have to choose between three different helicopter configurations, conventional, co-axial or tandem. After this decision, the *basic tool* operation will have minimal differences for each configuration in terms of the user experience, only the results will be significantly different.

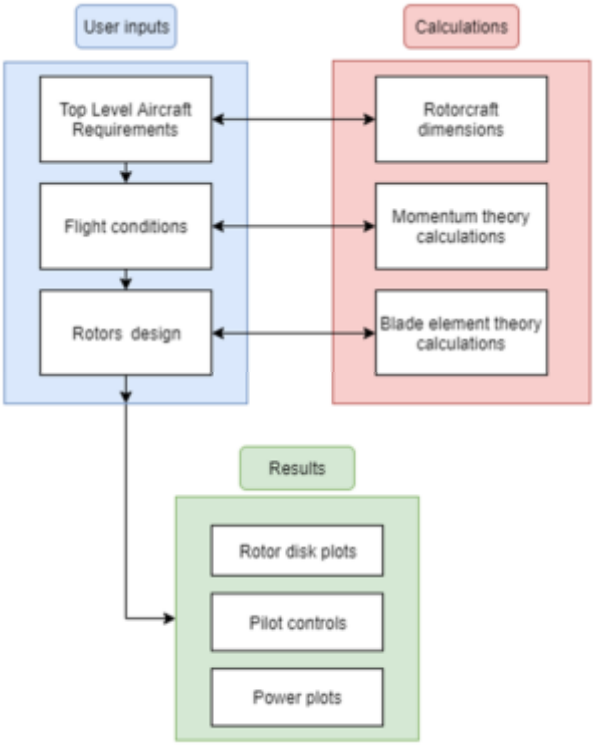

Figure 4: Basic tool structure

The user will be asked one single input to start the design of the chosen aircraft this input will be one of the following three (which one to choose is up to the user):

- Aircraft total mass – m in $[kg]$
- Number of passengers - N_{pass}
- Main rotor radius – R in $[m]$

With the one input the other two will be calculated. Based on the rotor radius the helicopter dimensions (both for the fuselage as for the rotors) are estimated using the relations from [4], that were extended to take into account the co-axial and tandem configurations.

Following the dimensions estimations, the user will define three flight conditions for the helicopter. The first calculations will follow the momentum theory, and the user will have the opportunity to generate a plot where the power variation with the forward velocity is shown.

After this, the rotors geometries might be set so that the blade element theory can be used and calculate a more accurate performance analysis of the helicopter. The variables that the user will be able to control in terms of the rotor design are:

- Number of blades - N_b
- Rotor radius – R

Presented at 46th European Rotorcraft Forum, Moscow, Russia, 8-11 September, 2020

- Rotor blade chord – c
- Rotor blade airfoil
- Rotor rotational velocity – Ω
- Rotor root-cut-out - r_0

The blade element theory calculation are used to trim the helicopter (in the conventional case taking into account the tail rotor contribution, and on the co-axial and tandem case taking into account the rotors' interaction).

The user has control over some of the calculations' parameters:

- Number of radial segments (radial discretization)
- Number of angular positions (azimuthal discretization)
- Convergence criteria
- Maximum number of iterations
- Linear inflow model

The results are demonstrated as rotor disk plots of the variable that the user wishes to see, and as power plots (showing the power variation with the helicopter flight velocity).

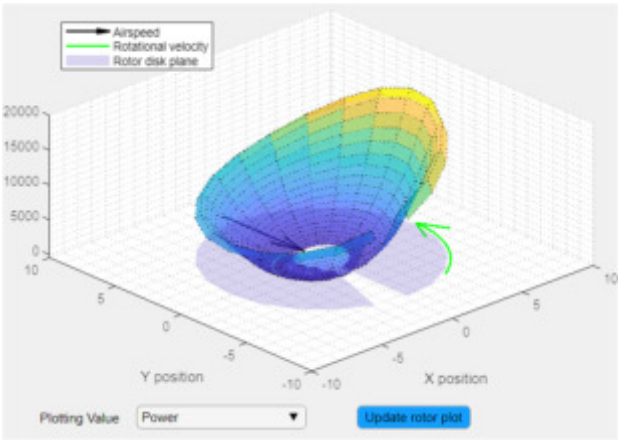

Figure 5: Basic tool – Main rotor disk plot

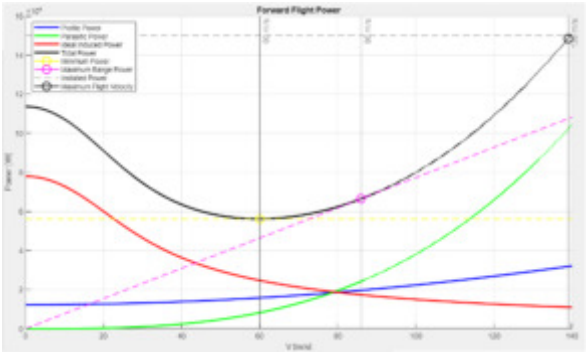

Figure 6: Basic tool – Power plot

3.2. Detailed tool

This tool offers a much deeper level of involvement in the helicopter design, more specific top level requirements can be defined, rotor blade geometry is now editable in terms of chord, twist and airfoil distribution along the blade, and a more complete rotor trim is introduced as the blade motion now also considers flapping (the pilot's cyclic controls will be calculated).

Figure 7: Detailed tool structure

The inputs required in regards to the top level aircraft requirements for this tool are:

- Aircraft payload - $m_{payload}$ in $[kg]$
- Crew and passengers - N_{pass}
- Cruise minimum range - R_{min} in $[km]$
- Cruise endurance – End in $[minutes]$
- Cruise speed - V_{cruise} in $[m/s]$
- Maximum gross weight – m_{gross}^{max} in $[kg]$

After having set all these values a series of calculations follow to assess the feasibility of the design.

The user will again be able to set some flight conditions and the result will be the generation of a design space where the disk loading (DL) *versus* the power loading (PL) will be plotted:

Presented at 46th European Rotorcraft Forum, Moscow, Russia, 8-11 September, 2020

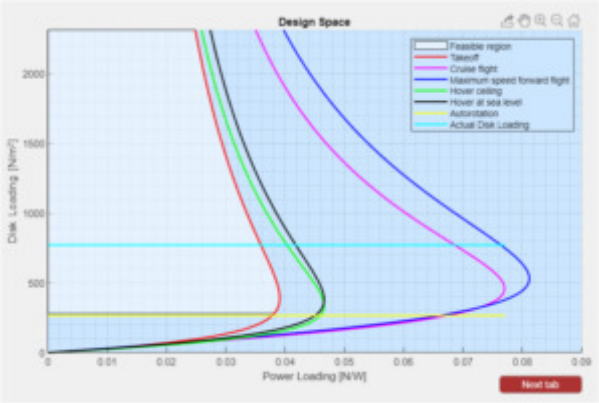

Figure 8: Design space

Following this, in the rotors geometry definition the user might change the variables shown below:

- Number of blades - N_b
- Rotor radius – R in $[m]$
- Rotor root cut-out - r_0 in [% of the rotor radius]
- Flapping hinge position - eR in [% of the rotor radius]
- Blade mass distribution in $[kg/m^2]$
- Rotor rotational velocity – Ω in $[rpm]$
- Chord distribution - $c(y)$ in $[m]$
- Twist distribution – $\theta(y)$ in [degrees]
- Airfoil distribution

The chord and twist distributions are continuous and the user can defined them as being constant, varying linearly or varying in a parabolic fashion along the blade span, furthermore the blade can be divided in up to three separate sections each one having a different airfoil (three section was found to be the common practice for helicopter blade design).

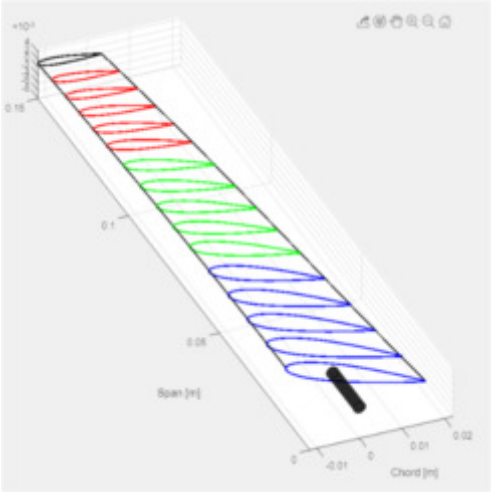

Figure 9: Rotor blade geometry example

The calculations parameters and the results representation in this tool are identical to what happens in the *basic tool*.

3.3. Additional configurations – rotor interaction

The user will have the freedom to choose to design a non-conventional helicopter (co-axial or tandem), the design process and tool structure is the same but the rotor calculations were adapted to account for the rotors interaction.

Depending on the configuration one of the rotors is assumed to work independently of the other (the top rotor for the co-axial and typically the front rotor for the tandem, but this depends on the specific configuration of the helicopter) and it's wake in the shedded onto the other rotor. Knowing the vertical and horizontal distance between the two rotors and the velocities in each point of the wake its contraction and translation are calculated to assess its area of influence in the bottom/rear rotor.

3.4. Drone tool

Through this tool the user will be able to design a multirotor unmanned aircraft of small dimensions.

Figure 10: Drone tool structure

The user inputs are:

- Fuselage body shape
- Number of rotors
- Coaxial or “single” rotor configuration
- Vertical spacing between coaxial rotors in $[m]$

Presented at 46th European Rotorcraft Forum, Moscow, Russia, 8-11 September, 2020

- Rotor arm in $[m]$
- Rotor radius in $[m]$
- Characteristic dimensions 1 and 2 in $[m]$
- Airframe material

The result of the user design is shown as a preliminary sketch:

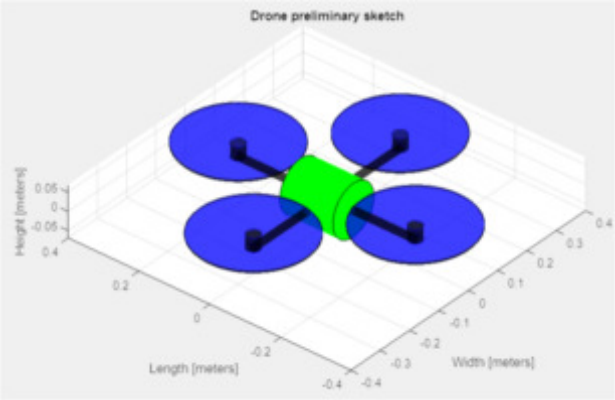

Figure 11: Drone preliminary sketch

The rotor design is identical to what has been described previously in section 3.2, and additionally the user will be able to define the material used on the rotor blades for weight estimation purposes.

After the geometry has been set, the flight performance requirements are needed:

- Payload and fuselage - $m_{payload}$ in $[kg]$
- Hover endurance - End_h in $[minutes]$
- Range in $[km]$
- Maximum velocity in $[m/s]$
- Flight ceiling in $[m]$

An assessment for the total mass of the aircraft based on the drone dimensions, airframe and rotor materials and flight conditions is done.

The process is iterative and is based on an initial estimation of the drone mass that is used to perform the calculations for the hover flight condition.

The airframe weight is calculated based on the material and its volume, the rotor blade weight is based on the rotor radius and the material used, the payload is defined by the user and these three components are fixed throughout the calculations. Torque and power requirements are calculated which may be related to the motor weight of each rotor and the total battery capacity (the propulsive system is assumed to be electric). After the calculations a new total mass is found and compared to the initial value. The process will continue until convergence given certain criteria.

After having defined all the geometric and weight characteristics of the drone the performance analysis might begin. The results will be shown as rotor disk plots and power plots (as is done in the *basic tool* and in the *detailed tool*).

3.5. Airfoil comparison tool

This is an extremely simple tool where the user can compare the 2-D aerodynamic performance of the available airfoils in the software database. Two different airfoils can be plotted as well as their C_l and C_d curves when varying the angle of attack. These curves are stored in a data base within the software and were generated using *XFOIL*, [12].

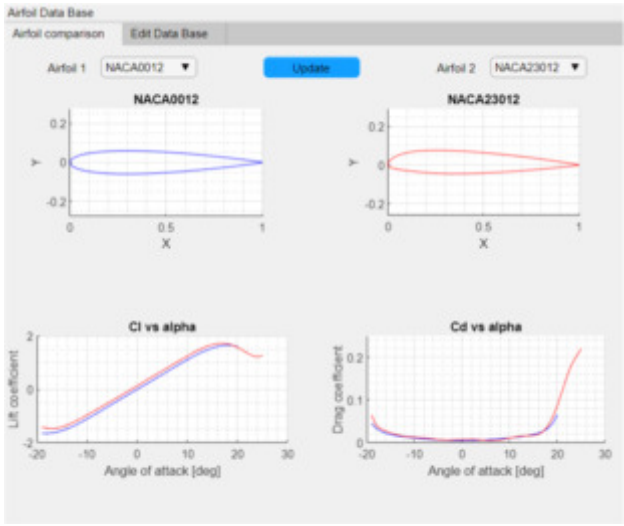

Figure 12: Airfoil comparison tool

4. VALIDATION

4.1. Sizing validation

The helicopter chosen for the validation process is the Sikorsky UH-60 Black Hawk. The geometric characteristics of the main and tail rotor used were obtained in [13].

To compare the results of the software for the helicopter dimensions the maximum take-off weight (MTOW) in kilograms was used as an input and the calculations were made from that starting point.

Presented at 46th European Rotorcraft Forum, Moscow, Russia, 8-11 September, 2020

Table 1: Conventional Helicopter dimensions validation

	Actual	Software
MTOW $[kg]$	8329.0	8329.0
Radius $[m]$	8.18	7.89
Height $[m]$	3.76	4.15
Length $[m]$	15.43	15.15
Tip to tip length $[m]$	19.76	18.66
Width $[m]$	2.95	2.98
Tail Rotor arm $[m]$	9.89	9.52

Table 2: Conventional Helicopter Main Rotor dimensions

	Actual	Software
Radius $[m]$	8.18	7.89
Blade chord $[m]$	0.53	0.52
Angular velocity $[rpm]$	27.00	28.47

Table 3: Conventional Helicopter Tail Rotor dimensions

	Actual	Software
Radius $[m]$	1.67	1.54
Blade chord $[m]$	0.25	0.21
Angular velocity $[rpm]$	124.62	127.34

The dimensions calculated using the software show a good agreement with the actual helicopter values.

4.2. Basic tool - performance

The rotor performance will be validated comparing the software results with the flight test data from [14].

The test flight were done considering an weight coefficient $C\_W = 0.0065$ which is equivalent to a $MTOW$ of 8329 kilograms at sea level.

$$(21)\ C_W = \frac{W}{\rho A V_{tip}^2}$$

with W being the aircraft weight, A the rotor disk area, and V_{tip} the blade tip velocity.

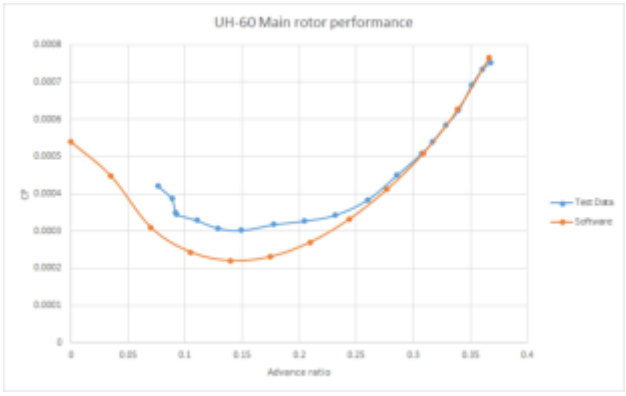

Figure 13: Main rotor power coefficient

Remembering that the inflow models are valid for $\mu > 0.15$ it is seen in Figure 13 that the results of the software are fairly acceptable given the low level of detail of the *basic tool*. The mean error was estimated interpolating the software calculated power requirements for the advance ratios considered on the flight test data and for the curves shown in Figure 13 was of 13.14%.

4.3. Detailed tool - performance

The same flight test data used above will be applied here to validate the values obtained using the *detailed tool*.

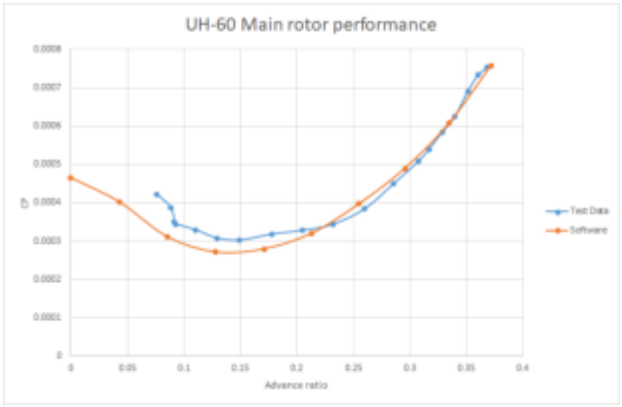

Figure 14: Main rotor power coefficient

It can be seen that the results when considering blade flapping (Figure 14) are in better concordance with the flight data when compared to the results in Figure 13, having reduced the mean error from 13.14% to 7.43%, this was expected as was stated before. The greatest improvements occur for low advance ratios making the results very close to the actual flight test values throughout the whole velocity range considered.

The consideration of the flapping motion allows for a trimming process of the helicopter to be done. The total inclination of the main rotor is easily calculated (estimating the aircraft drag for the longitudinal inclination, and calculating the tail rotor thrust for the lateral inclination in a conventional configuration) and this provides the attainment of

Presented at 46th European Rotorcraft Forum, Moscow, Russia, 8-11 September, 2020

more realistic results.

4.4. Co-axial configuration validation

To validate the analysis of a co-axial system a similar approach will be taken. Values from wind tunnel testing, see [15], will be compared to the software results.

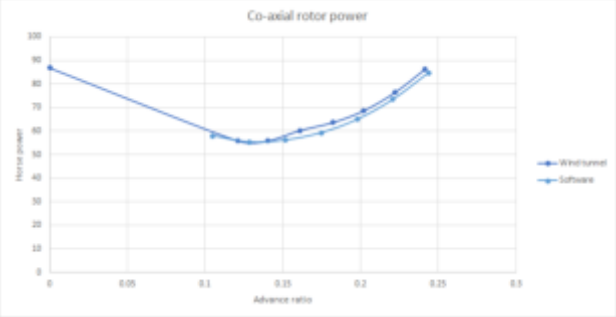

Figure 15: Co-axial rotor power

The results for the coaxial configuration (geometry described in [15]) show a good agreement between the software values and the wind tunnel test values.

4.5. Tandem configuration validation

Now performing a same type of analysis to a tandem rotor configuration and using wind tunnel test values from [15] the validation will be done.

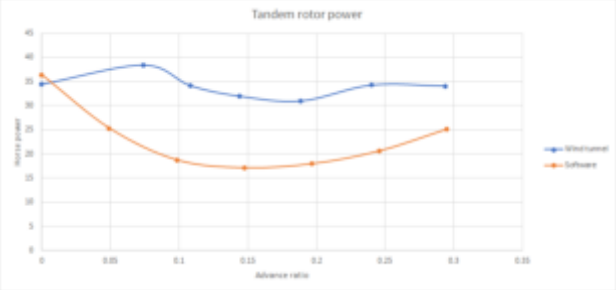

Figure 16: Tandem rotor power

The tandem configuration wind tunnel test results are somewhat scattered as is stated in [15], and the software calculated results are not close to the wind tunnel test ones, they follow a similar behaviour as do the results for a single or coaxial rotor.

This difference in the results might due to a low capability of analysing the interaction between the rotors, the presented configuration has no overlap and the two rotors are on the same plane, this means that in the software calculations no rotor wake will be shedded into the other rotor thus rendering them non interfering with which other.

4.6. Small dimensions rotor validation

A separate validation process was made for the drone rotors given the very reduced dimensions taken into account. The rotor considered is an 9 inch diameter propeller with a 6 inch pitch, the experimental values used on this process are from the work developed in [16].

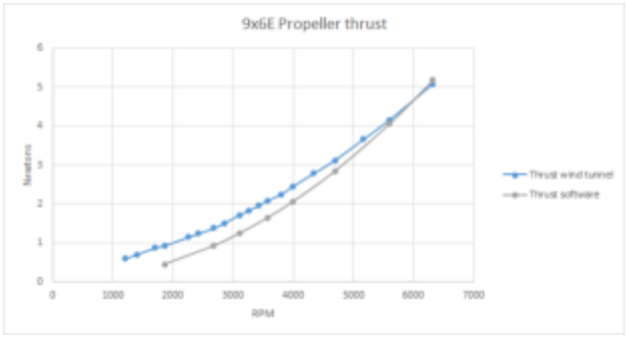

Figure 17: Propeller 9x6E thrust validation

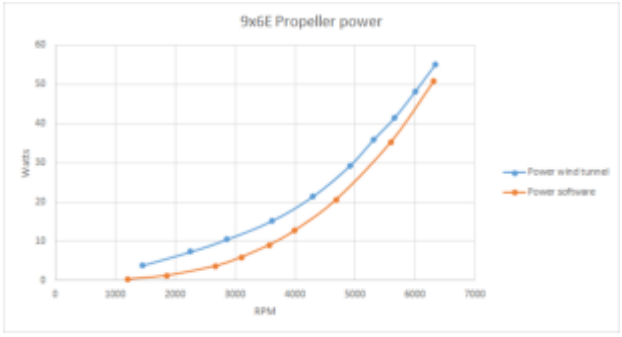

Figure 18: Propeller 9x6E power variation

4.7. Small dimensions co-axial validation

For the validation of the co-axial validation the top rotor was assumed not to be influenced by the presence of the lower rotor. Both rotors have equal rotational velocities in terms of magnitude but opposite directions. The vertical spacing between the top and bottom rotors was set at 52.2% of the rotor radius. The experimental results were once again obtained from the work [16].

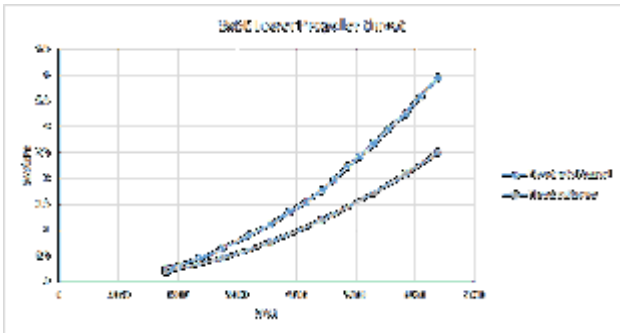

Figure 19: Propeller 9x6E thrust validation – Lower rotor

Presented at 46th European Rotorcraft Forum, Moscow, Russia, 8-11 September, 2020

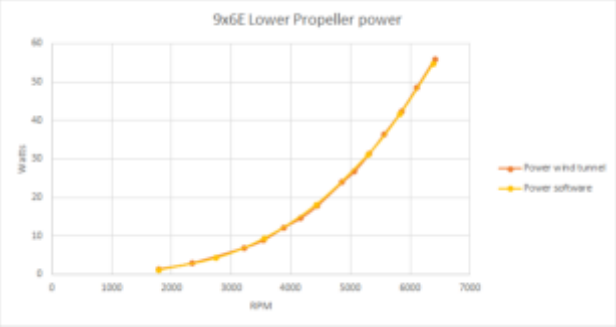

Figure 20: Propeller 9x6E power validation – Lower rotor

5. RESULTS

5.1. Helicopter – Conventional vs. Co-axial

In this section a direct software application will be demonstrated. Two different aircrafts (one conventional helicopter and one co-axial) with the same top-level requirements will be designed and the performances will be compared in order to choose the more viable solution.

Setting the aircraft requirements as:

Table 4: Top-level aircraft requirements

Top-level aircraft requirements	
Payload	10000 $[kg]$
Crew and passengers	20
Range	600 $[km]$
Endurance	300 $[minutes]$
Installed power	15000 [kW]

For both configurations, the initial weight estimation calculations are equal and the results for the total aircraft weight and fuel weight are the following:

Table 5: Weight estimation results

Fuel weight	5496 $[kg]$
Total aircraft weight	41500 $[kg]$

The general aircraft dimensions calculated for both configurations are:

Table 6: Dimensions results for the aircraft (with N/A meaning: not applicable)

	Conventional	**Co-axial**
Main rotor radius $[m]$	12.96	10.90
Height $[m]$	5.82	6.04
Length $[m]$	25.63	18.52
Tip to tip length $[m]$	31.15	24.50
Width $[m]$	4.22	4.76
Tail rotor arm $[m]$	16.14	N/A
Rotor vertical spacing $[m]$	N/A	1.50

The main rotor dimensions are:

Table 7: Dimensions results for the main rotor

	Conventional	**Co-axial**
Main rotor radius $[m]$	12.96	10.90
Blade chord $[m]$	1.24	1.24
Angular velocity $[rpm]$	18.85	21.76
Airfoil	*NACA4412*	*NACA4412*
Number of blades	4	4

The blades were designed as rectangular, untwisted and with the same airfoil throughout the span.

The tail rotor dimensions are:

Table 8: Dimensions results for the tail rotor

	Conventional
Tail rotor radius $[m]$	2.89
Blade chord $[m]$	0.77
Angular velocity $[rpm]$	75.53
Airfoil	*NACA4412*
Number of blades	2

Both aircrafts will be required to flight under the same set of conditions, which are:

Presented at 46th European Rotorcraft Forum, Moscow, Russia, 8-11 September, 2020

Table 9: Flight conditions

	Velocity $[m/s]$	Altitude $[m]$
Sea level hover	0	0
Maximum altitude hover	0	1250
Vertical climb	8	20
Cruise flight	35	500
Maximum velocity flight	45	50
Autorotational flight	10 (forward)	20

First the power requirements variation with the forward flight velocity at an altitude of 500 meters and an installed power value of 15000 kW for both helicopters will be evaluated, the calculations will use MT for an initial estimation.

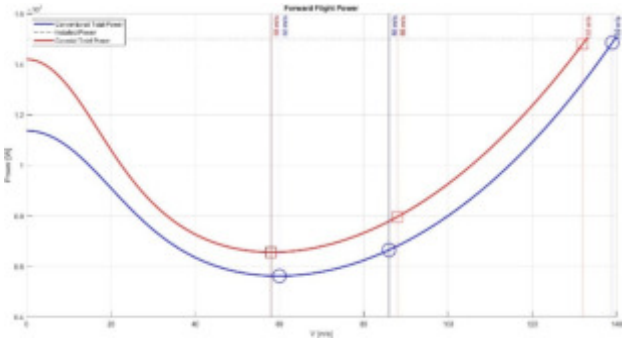

Figure 21: Conventional and co-axial helicopter configuration – Power curves

Table 10: Performance results using MT for both configurations

	Conventional	**Co-axial**
Maximum power velocity $[m/s]$	60	58
Maximum power for level flight $[kW]$	5619.4	6560.7
Maximum range velocity $[m/s]$	86	88
Maximum forward velocity $[m/s]$	139	132

Note: These results were obtained using MT and show an approximation of the power curves for both configurations.

The two configurations show similar results for the minimum power flight velocity, maximum range velocity and maximum forward velocity. The major difference is in terms of the power for maximum range where a difference of almost 17% with the co-axial configuration consuming more power.

The velocity values calculated for the minimum power flight are both higher than the velocity for the maximum velocity flight conditions specified in the Table 9.

Now both configurations will be analysed, using BET and considering the flapping motion, for each of the flight conditions presented and their performances will be compared.

Table 11: Flight performance comparison

	Conventional power $[kW]$	**Co-axial power $[kW]$**
Sea level hover	9652.7	10756.5
Maximum altitude hover	10062.4	11087.6
Vertical climb	14623.0	14749.1
Cruise flight	5098.8	4767.2
Maximum velocity flight	4616.1	4237.3

For the autorotational flight the power is null (by definition of the flight condition) so the result to be looked at is the descent velocity that allows for the helicopter to operate in autorotation. For the conventional case, this result was a descent velocity of 19.24 $[m/s]$ and for the co-axial case is was of 25.32 $[m/s]$, which represents a difference of 31.6%.

Note: These results were obtained using BET, so they differ from the ones presented in Table 10.

It is noted in Table 11 that the co-axial configuration is less efficient when looking at axial flight conditions, but for these specific cases (geometry, dimensions, and flight characteristics) the co-axial helicopter requires less power for the level flight operations (cruise and maximum velocity).

It can also be seen that the power required for the maximum velocity flight is lower than the power for the cruise flight (for both configurations) which means that that velocity value is on the descendent part of the power curve and the minimum power flight conditions is yet to be found.

5.2. Drone

Two different case studies were done using the drone tool to compare two main aspects of the

Presented at 46th European Rotorcraft Forum, Moscow, Russia, 8-11 September, 2020

drone design, the number of rotors and the rotor configuration (single or co-axial).

Some of the characteristics remained constant for all the drones designed as is specified in Table 12 (geometric details) and Table 13 (performance requirements).

Table 12: Drones' geometric characteristics

Geometric characteristics	
Fuselage shape	Cube
Cube side length	0.1 $[m]$
Rotor arm	0.3 $[m]$
Number of blades per rotor	2
Rotor radius	0.15 $[m]$
Rotor blade chord	0.03 $[m]$

Table 13: Drones' flight requirements

Flight requirements	
Payload	0.7 $[kg]$
Hover endurance	20 $[minutes]$
Flight ceiling	100 $[m]$
Maximum velocity	30 $[m/s]$

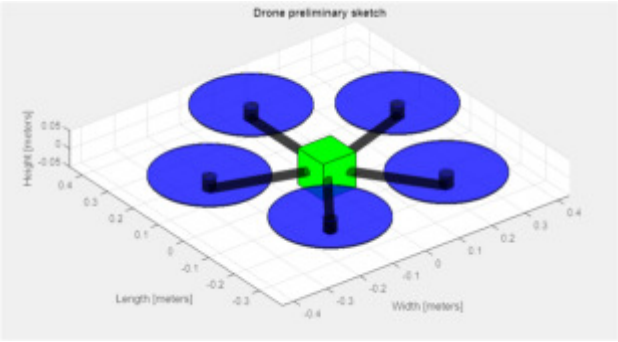

Figure 22: 5 rotor drone

5.2.1. Number of rotors

Three different drones were designed varying the number of rotors (3, 4, and 5 rotors) to evaluate the impact of this aspect on the aircraft weight and performance.

Table 14: Drones' Weight Breakdown

Weight breakdown $[kg]$			
	3 rotors	4 rotors	5 rotors
Airframe	0.440	0.586	0.733
Motors	0.124	0.126	0.133
Batteries	0.985	0.885	0.874
Payload	0.700	0.700	0.700
Rotor blades	0.037	0.050	0.062
Total	2.286	2.347	2.502

Table 15: Drones' Hover performance

Hover performance			
	3 rotors	4 rotors	5 rotors
Power $[W]$	221.3	246.2	218.6
Total Energy $[kJ]$	295.4	265.6	262.3
Rotors' RPM	4005.5	3515.7	3252.2

The airframe and rotor blades weights are directly linked to the number of rotors used and it can be seen in Table 14 that they vary linearly. The battery weight decreased with the addition of rotors (for these specific cases), this is a result of the lower force generating requirements of each rotor which allows them to operate at lower rotational velocities decreasing the total drag and consequently the power.

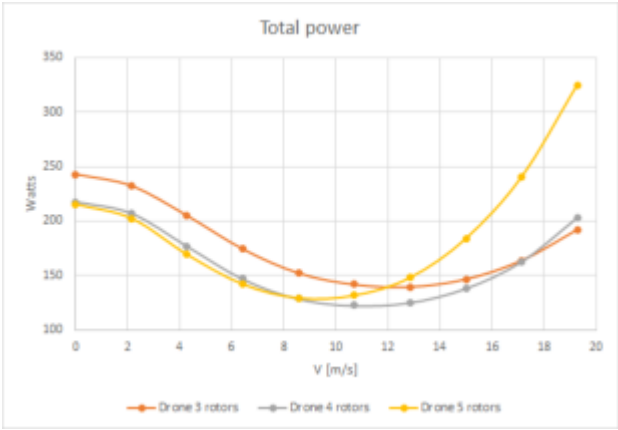

Figure 23: Total power variation with the forward velocity

Figure 23 shows the power requirements variation with the forward velocity for the three drones designed. It can be observed that the

Presented at 46th European Rotorcraft Forum, Moscow, Russia, 8-11 September, 2020

increase in the number of rotors provides better performance (less power is required) for the low velocity range, this is a result of lower induced and profile power due to lower rotational velocities, but with the increase of the flight velocity, given the airframe necessities associated with the number of rotors, the parasitic drag increases much more for the drones with more rotors thus compromising their performance for higher flight velocities.

5.2.2. Rotor configuration

Now the rotor configuration will be evaluated. Two drones were generated, one with 4 rotors and another with 4 pairs of co-axial rotors.

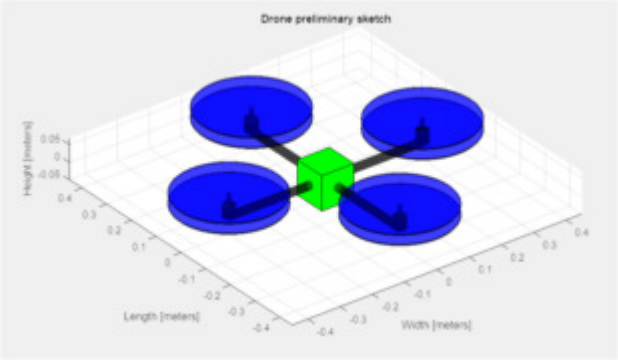

Figure 24: 4 co-axial rotors drone

The geometric characteristics and flight requirements are the same as stated in tables 12 and 13.

Table 16: Drones' Weight Breakdown

Weight breakdown [kg]		
	Single	Co-axial
Airframe	0.586	0.586
Motors	0.124	0.228
Batteries	0.885	1.865
Payload	0.700	0.700
Rotor blades	0.050	0.100
Total	2.347	3.479

Table 15: Drones' Hover performance

Hover performance		
	Single	Co-axial
Power [W]	246.3	466.4
Total Energy [kJ]	265.6	559.7
RPM (top)	3515.7	3015.8
RPM (bottom)	N/A	-3874.0

The hover performance of the co-axial configuration is much more power demanding which increases the battery capacity and consequently the total drone weight.

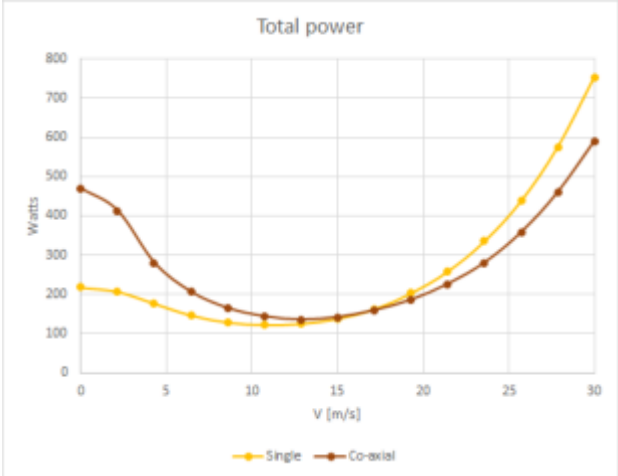

Figure 25: Total power variation with the forward velocity

For forward velocities inferior to 15 [m/s] the co-axial configuration has higher power requirements due to higher values of induced power, but this component decrease more rapidly with the flight velocity in this configuration and so for higher velocities the co-axial total power is lower.

Note: The parasitic power of both configurations is the same throughout these calculations.

6. CONCLUSIONS

6.1. Achievements

This work set out to provide a free, open source, user friendly computational tool for the design of rotary wing aircrafts of different configurations.

The results presented in section 4 are the proof that the software is capable of providing quality results very quickly and of presenting them in a clear manner so that the user can evaluate the design impacts of the aircraft performance.

Presented at 46th European Rotorcraft Forum, Moscow, Russia, 8-11 September, 2020

The results obtained for the UH-60 were extremely good, as is shown in Figure 14, and there was a significant improvement when comparing with the results where no flapping was considered, see Figure 13.

For the co-axial configuration both helicopter rotors and small drones' rotors were considered both showing good results as is demonstrated in Figure 15 for the helicopter case, and in Figures 19 and 20 for the drone case.

The versatility of the tool is clearly demonstrated in section 5 where different helicopter and drone designs are obtained using the same requirements as starting points. This is the perfect example of the applicability of this software as the user can easily and quickly design different helicopters, compared the results (dimensions and performance) and from that point chose what is most suitable for their specific case.

The work developed here is shown to be a very viable and useful tool and its open source nature makes it all the more attractive for the people interested.

6.2. Software availability

The software tool is available with the source code at: https://github.com/tomaspfontes/RotorcraftDesignTool

6.3. Acknowledgments

This work was supported by FCT, through IDMEC, under LAETA, project UIDB/50022/2019.

6.3.1. References

[1] – Roman Vasylioviych Rutskyy. Desenvolvimento de uma ferramenta computacional para projecto preliminar do helicóptero de configuração convencional. Masters' thesis, Instituto Superior Técnico, 2014.

[2] – Anatol Conjocari. Preliminary design tool of conventional/coaxial/tandem helicopters. Masters' thesis, Instituto Superior Técnico, 2016.

[3] – Miguel Ponte. Development of a Preliminary Design Tool for Conventional Co-axial and Tandem Helicopter Configurarion. Masters' thesis, Instituto Superior Técnico, 2016.

[4] - Rand Omri and Khromov Vladimir. Helicopter Sizing by Statistics. In *American Helicopter Society 58th Annual Forum*, 2002.

[5] - J. Gordon Leishman. *Principles of Helicopter Aerodynamics*. Cambridge University Press, 2006.

[6] - Coleman R. P, Feingold M. A, and Stempin C. W. Evaluation of the Induced Velocity Fields of an Idealized Helicopter Rotor. Technical report, NACA ARR L5E10, 1945.

[7] - Drees J. M. A Theory of Airflow Through Rotors and Its Application to some Helicopter Problems. *Journal of the Helicopter Association of Great Britain*, 3 (2):pp 79-104, Jul-Set, 1949.

[8] - Payne P. R. *Helicopter Dynamics and Aerodynamics*. Pitman & Sons, London, 1959.

[9] - White F. and Blake B. B. Improved Method of Predicting Helicopter Control Response and Gust Sensitivity. In *35th Annual Forum of the American Helicopter Society, Washington DC, Washington DC,* 1979.

[10] - Pitt D. M. and Peters D. A. Theoretical Predications of Dynamic Inflow Derivatives. *Vertica,* 5:pp 21 34, 1981.

[11] - Howlett J. J. UH-60 Blackhawk Engineering Simulation Program: Vol. 1 - Mathematical Model. Technical report, NASA CR-66309, 1981.

[12] - XFOIL Subsonic Airfoil Development System. URL: https://web.mit.edu/drela/Public/web/xfoil/. Consulted on July, 2020.

[13] - Dong Han, Vasileios Pastrikakis, George N. Barakos. Helicopter performance improvement by variable rotor speed and variable blade twist. *Aerospace Science and Tecnhology*, 2016.

[14] - Wayne Johnson, William G. Bousman, Hyeonsoo Yeo. Performance Analysis of a Utility Helicopter with Standard and Advanced Rotors. In *American Helicopter Society Aerodynamics, Acoustics, and Test and Evaluation Technical Specialist Meeting*, 2002.

[15] - Richard C. Dingeldein. Wind-Tunnel Studies of the Performance of Multirotor Configurations. Technical report, NACA TN 3236, Langley Field, VA, 1954.

[16] - Inês Silva Amado. Experimental Comparison of Planar and Coaxial Rotor Configurations in Multi-rotors. Masters' thesis, Instituto Superior Técnico, 2017.

Presented at 46th European Rotorcraft Forum, Moscow, Russia, 8-11 September, 2020